The Capture Efficiency of Coated Voids

W.G. Wolfer and L.K. Mansur

November 1979

UWFDM-329

J. Nucl. Matls. 91, 265-276 (1980).

FUSION TECHNOLOGY INSTITUTE

UNIVERSITY OF WISCONSIN

MADISON WISCONSIN

The Capture Efficiency of Coated Voids

W.G. Wolfer and L.K. Mansur

Fusion Technology Institute
University of Wisconsin
1500 Engineering Drive
Madison, WI 53706

http://fti.neep.wisc.edu

November 1979

UWFDM-329

J. Nucl. Matls. 91, 265-276 (1980).

The Capture Efficiency of Coated Voids

W. G. Wolfer
Nuclear Engineering Department
University of Wisconsin
Madison, Wisconsin 53706 U.S.A.

and

L. K. Mansur
Metals and Ceramics Division
Oak Ridge National Laboratory
Oak Ridge, Tennessee 37830 U.S.A.

November 1979

UWFDM-329

Abstract

The segregation of impurities and alloying elements to voids is considered to play an important role in radiation-induced swelling in structural materials. Following an earlier proposal, it is shown that when segregation causes a small change in the elastic properties of the material around the void, called the shell, the mechanical interaction between point defects and the void is significantly affected. The entire mechanical interaction contains several contributions: the change in the relaxation energy of the point defect, the modification of its image interaction, the long-ranged stress-induced interaction, and an interaction due to coherency strains when segregation also produces changes in the lattice parameter. A detailed discussion of all these contributions is given.

An activation barrier for point defect diffusion is created in the shell when its shear modulus is somewhat larger than in the matrix, or when coherency strains are present. In the absence of the latter the activation barrier is mainly produced by the difference of the relaxation energies between shell and matrix, whereas the image interaction mainly effectuates a smooth transition for the otherwise discontinuous change in the relaxation energy. If the shear modulus of the shell is smaller than in the matrix, a barrier is only produced by coherency strains.

It is argued that the sum of the relaxation and the image interaction energies of a crystal defect must change in a continuous way through a coherent interface. By virtue of this requirement, divergences and ambiguities in the image interaction can be removed.

The exact expressions for the image interaction involve slowly converging sums. In order to facilitate their use, simple and sufficiently accurate approximations are developed for them. It enables us to derive concise expressions for the energy barrier of the shell and the capture efficiency of voids. Specific numerical examples are given for this capture efficiency of voids with surface coatings or impurity shells. It is found that the capture efficiency for interstitials is more strongly affected than for vacancies. Voids with shells become biased against interstitials. The importance of these results to void nucleation and swelling is discussed.

I. Introduction

Current experimental research has shown that impurity and alloying element content have a strong influence upon the swelling behavior of metals [1,2]. This fact has great significance for the development of low swelling alloys to be used in structural components of future fission and fusion reactors. To make such development systematic it is necessary to understand the basis of impurity action. In light of our current understanding of swelling [3], impurities may act in two ways. First, by altering the free migration of point defects in the material through trapping reactions and, second, by changing the relative capture efficiencies of point defects at sinks, such as voids, dislocations and precipitates. The former effect has often been invoked in speculative explanations of differences in swelling behavior, but has received more detailed attention recently [4]. However, we believe it is important to investigate physical mechanisms for the latter possibility also since swelling depends so delicately on small differences in the point defect capture efficiencies of the sinks in the swelling material [3].

Solute segregation to void surfaces in stainless steels [5] and aluminum [6] has been observed. Furthermore, segregation to void surfaces is expected to occur widely in light of observations of segregation on virtually all free surfaces. This is thought to be due to the usual lowering of the thermodynamic free energy of the system as well as to impurity coupling to radiation-induced point defect fluxes of vacancies and interstitials. It is important to answer the question as to what effects such segregation may have on the efficiency with which a void absorbs point defects and ultimately on swelling. By altering the diffusion coefficients

of point defects near the void, a segregated layer may affect swelling. This has been explored by Brailsford [7]. As first proposed by Wolfer [8], a further mechanism by which a segregated layer may affect swelling behavior is through alteration of the point defect-void image interaction. The purpose of this paper is to describe the results of a continued study of this effect which was previously reported in Refs [9,10].

In the present paper we restrict ourselves to the detailed discussion of the interaction energy of point defects with coated voids and to a computation of the void capture efficiency. This is carried out in Sections II and III, respectively. The numerical evaluation of the void capture efficiencies for interstitials and for vacancies follows in Section IV. The results and their significance to void formation are discussed briefly in Section V.

II. The Interaction Energy of Point Defects with Coated Voids

Segregation of solute elements, now recognized as a common phenomenon occurring under irradiation, produces a non-uniform composition. Since the elastic properties depend on composition, the elastic moduli exhibit a spatial variation also. In turn, the elastic properties affect the local formation energy of the point defect, and in the case of a void, they also affect the long-range mechanical interaction between the point defect and the void surface. The latter interaction has been derived previously by Wolfer and Mansur [11] and applied to void nucleation and growth [9,10]. However, the former effect, namely the change in the formation energy of the point defect was not included in our previous investigations nor in investigations by other authors dealing with problems of the image interaction in general. It will be shown in this section that the change in

formation energy is of greater importance to the quantitative evaluation of the void capture efficiency than the image interaction. Furthermore, the physical basis for a surface barrier to point defect absorption at voids is to be found in the change of the formation energy rather than the image interaction. In spite of these differences, however, our former conclusions [9,10] based on the image interaction alone remain qualitatively correct.

When considering the diffusion of point defects with local concentrations $C(\underset{\sim}{r})$ in an elastically deformed lattice, the diffusion flux

$$\underset{\sim}{j} = - \underset{\sim}{\nabla}(DC) - DC \frac{1}{kT} \underset{\sim}{\nabla} U^S \qquad (1)$$

contains a drift term, the second term in Eq. (1). It depends on the spatial variation of the saddle-point energy, $U^S(\underset{\sim}{r})$ of the point defect, as indicated schematically in Fig. 1. Here, the dashed line represents the potential energy of a point defect as it migrates in an ideal lattice, whereas the solid line shows the potential energy in a deformed lattice. Potential energy changes between the deformed and the ideal lattice are henceforth designated by U with a superscript S or F for the saddle-point or the stable configuration. The particular form of the drift term in Eq. (1) arises because of the assumption that the diffusion coefficient for migration, D, depends on the local lattice deformation according to the equation

$$D(\underset{\sim}{r}) = D^0 \exp[-U^M(\underset{\sim}{r})/kT] \quad , \qquad (2)$$

where D^0 is the value of the diffusion coefficient in an unstrained lattice.

The change of the activation energy for migration is given by

$$U^M(\underset{\sim}{r}) = U^S(\underset{\sim}{r}) - U^F(\underset{\sim}{r}) \quad , \tag{3}$$

where $U^F(\underset{\sim}{r})$ is the change of the formation energy of the point defect in its stable configuration. The energies U^S and U^F can be derived from the same expressions for the interaction energy of the point defect with the void, provided we know the relaxation volume, v, and the elastic polarizabilities, α, of the point defect in both its saddle-point and its stable configuration. In reality, we must assume that these parameters are the same for both configurations, since only those for the stable configuration are presently known.

There are three contributions to the interaction energy, and hence to U^S. The first is due to the long-range mechanical interaction of the point defect with an interface or a free surface, and it is referred to as the image interaction $U^I(\underset{\sim}{r})$. The second long-range contribution, $U^\sigma(\underset{\sim}{r})$, arises from the interaction of the point defect with the stress field generated by the void itself with or without an externally applied load. Both contributions, U^I and U^σ, being of mechanical origin, can be evaluated with the help of elasticity theory and with models for point defects treating them as centers of dilation and inhomogeneous inclusions.

The third contribution arises from the local lattice properties such as density, composition, and elastic moduli. This contribution will be referred to as the relaxation energy, $U^R(\underset{\sim}{r})$, of the point defect.

In the following, we will consider these three contributions for the case of a spherical void of radius r_s coated with a shell of thickness

$h = r_m - r_s$ whose elastic properties are different from those of the matrix material. In the previous evaluation of the image interaction, U^I, it was found [11] that the difference in the Poisson ratios for the shell, ν_s, and the matrix, ν_m, had little effect on U^I. Hence, we assume that $\nu_s = \nu_m = \nu$, and that only the shear moduli μ_s and μ_m differ.

To express the image interaction U^I in an exact form requires an infinite series which converges slowly. Although the exact form was used earlier [9,10] it was shown previously [11] that sufficiently accurate approximations can be found which are more convenient to use.

For example, if the point defect is within a distance of a few shell thicknesses from the interface, the image interaction of the point defect in the matrix at a radial distance $r > r_m$ from the void center can be approximated by

$$U_m^I(r) \cong \frac{\Gamma_m}{4(1-\nu)-1+g}\left[\frac{(1-g)}{(r-r_m)^3} - \frac{16g(1-\nu)^2}{4g(1-\nu)-1+g}\frac{1}{(r-r_s)^3}\right] . \qquad (4)$$

On the other hand, inside the shell where $r_s \leq r \leq r_m$, the image interaction can be approximated by

$$U_s^I(r) \cong -\Gamma_s\left\{\frac{1}{(r-r_s)^3} + \frac{(1-g)}{4g(1-\nu)+1-g}\left[\frac{r/r_m}{(r_m-r)^3} - \frac{2r_m/r}{(r_m-r_s)^3}\right]\right\} . \qquad (5)$$

In these two equations

$$g = \mu_m/\mu_s \quad , \qquad (6)$$

and

$$\Gamma = v^2 \mu \frac{(1+\nu)^2}{36\pi(1-\nu)} \quad , \qquad (7)$$

where v and μ assume the values v_m and μ_m or v_s and μ_s, respectively, according to the subscript on Γ.

In Eq. (4), the second term represents the image interaction with the void surface, but modified because it is transmitted through the shell, whereas the first term is the image interaction with the interface. Similarly, the first term in Eq. (5) approximates the image interaction of the point defect with the void surface, whereas the second and third term represent the image interaction with the interface. Eq. (5) is sufficiently accurate for a thin shell, i.e., when $(r_m - r_s) \ll r_s$.

At both the free surface and the interface these expressions for U^I diverge, as do the exact ones. This mathematical artifact arises because the point defect is treated as a mathematical point. In reality, of course, its extent is of the order of the atomic radius, and the above expressions for U^I are valid only up to a distance of closest approach. This distance of closest approach could not be determined precisely in our previous work [9,10], and it was chosen as the atomic radius or one-half of the Burgers vector.

By including the relaxation energy into the analysis, it is now possible, as shown below, to determine the distance of closest approach from the requirement that the strain energy of the point defect change continuously and monotonically when crossing an interface.

The strain energy associated with a point defect far away from external surfaces or interfaces is determined by the relaxation of the surrounding atoms upon creation of the defect. According to Eshelby [13], this so-called relaxation energy or self-energy can be written as

$$U^R = \frac{2}{9} \mu \frac{1+\nu}{1-\nu} \frac{v^2}{\Omega} = \frac{8\pi}{1+\nu} \frac{\Gamma}{\Omega} \quad , \tag{8}$$

where Ω is the atomic volume.

The total strain energy of the point defect is now the sum of U^R and U^I. It is now argued that this total strain energy (U^R+U^I) must be a continuous function even in a heterogeneous medium. We can rationalize this by considering first a heterogeneous material with no sharp interfaces, such as a spinoidally decomposed alloy. Although the strain energy associated with a defect varies with location, it does so in a continuous and smooth manner. Next, we suppose that the spinoidal decomposition leads finally to a formation of a new phase in the form of coherent precipitates. As the new phase emerges gradually from the spinoidal concentration variations, the strain energy remains always a continuous and smooth function.

Based on this reasoning, it is required that $(U^R + U^I)$ change continuously across any coherent interface, and in the extreme, even across a free surface. It will become evident shortly that this requirement also ensures the monotonic change of $(U^R + U^I)$. Furthermore, it will enable us to determine in a consistent and clearly defined way the distances of closest approach, up to which the expressions for U^I are applicable. Let us first apply these ideas to the free void surface. As the point defect reaches this surface its total strain energy disappears, and it is dissipated as thermal vibrations of the surrounding atoms. We may imagine that the defect energy is zero inside the void.

The distance of closest approach, d_o, to the void surface is then defined by the condition

$$U_s^R + U_s^I(r_s + d_o) = 0 \quad . \tag{9}$$

Using Eqs. (8) and (5), we obtain

$$\frac{\Omega}{d_o^3} \cong \frac{8\pi}{1+\nu} + \frac{(1-g)}{4g(1-\nu)+1-g}\frac{\Omega}{h^3} \tag{10}$$

where

$$h = r_m - r_s \tag{11}$$

is the shell thickness. To obtain the Eq. (10), it was assumed that $r_m - r_s - d_o \cong r_m - r_s = h$ and that $(r_s + d_o)/r_m \cong 1$. When the shell thickness is greater than a few atomic distances, then $\Omega/h^3 << 1$, and the last term in Eq. (10) can be neglected. One obtains then the distance of closest approach to a flat surface on a homogeneous material, namely [13]

$$d_o = \left(\frac{1+\nu}{8\pi}\,\Omega\right)^{1/3} . \tag{12}$$

Next, we determine the distance of closest approach, d, to the interface in a similar fashion. Accordingly, we require that

$$U_m^R + U_m^I\,(r_m+d) = U_s^R + U_s^I(r_m-d) , \tag{13}$$

where U_m^R and U_s^R are the relaxation energies in the matrix and shell, respectively. Upon using the expressions in Eqs. (4), (5), and (8), and solving Eq. (13) for d, a rather lengthy formula is obtained. We may simplify it by neglecting terms of the order of Ω/h^3 and of order d/h. The result can then be written in the form

$$d \cong \{\Omega\,\frac{1+\nu}{8\pi}\,|\,\frac{1-g}{\Gamma_s-\Gamma_m}\,|\,[\frac{\Gamma_s}{4g(1-\nu)+1-g} + \frac{\Gamma_m}{4(1-\nu)-1+g}]\}^{1/3} . \tag{14}$$

A note of caution is in order here. The equation cannot be used for the pathological case where $\Gamma_s = \Gamma_m$ and $g \neq 1$, because the terms of order Ω/h^3 can no longer be neglected. However, for the case with $g = 1$ (or $\mu_s = \mu_m$), Eq. (14) does predict the correct result, namely $d = 0$.

The significance of the results obtained is demonstrated in Fig. 2 for a case, not believed to be typical of coated voids, but chosen for a clear illustration of the concept of a surface barrier. The shear modulus of the shell is taken as $\mu_s = 2\mu_m$, and the relaxation volumes are selected to be equal, $v_s = v_m$, so that $\Gamma_s = \Gamma_m/g$. The solid line in Fig. 2 represents the total strain energy $(U^R + U^I)$ of the point defect. The dotted lines are the total strain energies $(U_m^R + U_o^I)$ and $(U_s^R + U_o^I)$, representing the two cases of uncoated voids in materials with shear moduli μ_m and μ_s, respectively. Here, U_o^I is the image interaction for a bare void. The plateau in the vicinity of the interface is a result of the self-consistent procedure to find the distance of closest approach. It is an artifact which arises because the interface is treated as a mathematical surface and the point defect as a mathematical point. The conjectured physical behavior of $(U^R + U^I)$ is indicated by the dashed line. The presence of this plateau has no effect on the void capture efficiency, however, as will become evident in the next section.

As this example in Fig. 2 shows, the image interaction alone does not by itself produce the surface barrier. Rather, it is the difference in the relaxation energies, $U_s^R - U_m^R$, which is the primary cause for the surface barrier. The image interaction close to the interface merely produces a gradual transition for the otherwise discontinuous jump in the relaxation energy U^R. Furthermore, the image interaction U_o^I with the bare void smooths out the jump from U_s^R to zero at the void surface.

It is now obvious from this discussion that a soft shell, with $\mu_s < \mu_m$ and $U_s^R < U_m^R$, produces no surface barrier, in contrast to previous results based on the image interaction alone [9,10,11].

The illustrative example of Fig. 2 suggests further approximations which will be convenient for the subsequent evaluation of the void capture efficiency. The total strain energy $(U^R + U^I)$ can be divided into a long-range part upon which is superimposed a short-range "shell barrier" which we approximate by a constant value ΔU^o.

The long-range part is nearly identical with the image interaction of a bare void, U_o^I. Its exact expression is again given in the form of an infinite series. For convenience, however, we develop a simple approximate expression in the following way. At large distances r from the void center, U_o^I has an r^{-6} leading term. At distances close to the void surface, U_o^I is proportional to $(r-r_s)^{-3}$. We combine these two extremes in the following form

$$U_o^I(r) \cong -\frac{\Gamma_m}{r_s^3}\left\{\left(\frac{r}{r_s} - 1\right)^3 + \frac{7-5\nu}{30}\left(\frac{r}{r_s} - 1\right)^6\right\}^{-1} \quad . \tag{15}$$

The comparison between this approximate form and the exact one for U_o^I in Fig. 3 demonstrates the good agreement.

For the short-ranged part we replace the spatial variation of the shell barrier energy

$$\Delta U(r) = U_s^R - U_m^R + U_s^I(r) - U_o^I(r) \tag{16}$$

by a constant value ΔU^o. Since $\Delta U/kT$ appears later on in an exponential when computing the capture efficiency, we choose the maximum value of

$\Delta U(r)$ as the effective barrier height ΔU^o. If we further assume that $h \ll r_s$, Eq. (5) can be written as

$$U_s^I(r) \cong - \Gamma_s \{\frac{1}{(r-r_s)^3} + \frac{(1-g)}{4g(1-\nu)+1-g} [\frac{1}{(r_m-r)^3} - \frac{2}{h^3}]\} \tag{17}$$

and Eq. (15) as

$$U_o^I(r) \cong - \Gamma_m/(r-r_s)^3 \ . \tag{18}$$

By solving the equation $d\Delta U/dr = 0$ we find that the maximum of ΔU is located at $r_s + \rho$, where

$$\rho = h/(1+B^{1/4}) \tag{19}$$

and

$$B = \frac{(1-g)}{4g(1-\nu)+1-g} \frac{\Gamma_s}{\Gamma_s-\Gamma_m} \ . \tag{20}$$

The maximum value of ΔU is given by

$$\Delta U^o = \Delta U(r_s+\rho) = \frac{(\Gamma_s-\Gamma_m)}{\Omega} \{\frac{8\pi}{1+\nu} - \frac{\Omega}{h^3} [(1+B^{1/4})^4 - 2B]\} \ . \tag{21}$$

The first term represents the difference in the relaxation energies U_s^R and U_m^R, while the second one is due to the difference in the image interactions U_s^I and U_o^I within the shell.

In the following, we assume that the difference in the relaxation energies is only due to the differences in the shear moduli. Then, $\Gamma_m/\Gamma_s = g$, and

$$\Delta U^o = \frac{\Gamma_m}{\Omega} (\frac{1}{g} - 1)\{\frac{8}{1+\nu} - \frac{\Omega}{h^3} [(1+B^{1/4})^4 - 2B]\} \tag{22}$$

with

$$B = 1/[4g(1-\nu)+1-g] \quad . \tag{23}$$

Using the parameters listed in Table 1 and Eq. (7), $(\Omega/v_s)^2 \Delta U^o$ can be computed according to Eq. (22). The results are shown in Fig. 4 as a function of (1-g) and for different values of (h^3/Ω). For a modulus difference of only 2% and for the relaxation volumes given in Table 1, we find that the shell barrier is about 0.2 eV for the interstitial, and 0.004 eV for the vacancy.

Also shown in Fig. 4 is the image interaction U_o^I at $r = r_s + \rho$, which is given by

$$U_o^I(r_s+\rho) = - \Gamma_m/\rho^3 = - \Gamma_m(1+B^{1/4})^3/h^3 \quad . \tag{24}$$

It is seen that U_o^I is small in comparison with ΔU^o when $h^3 >> \Omega$. Nevertheless, because of the long-range action of the image interaction U_o^I, it is found to play an important role in the void capture efficiency.

There can be two more contributions to the barrier inside the shell. The first one arises from coherency strains if a lattice parameter mismatch exists between the shell and matrix materials. If the lattice parameter in the shell is greater by Δa, the point defect changes its energy in the shell by the additional amount

$$\Delta U^c = 2\mu_s \frac{1+\nu}{1-2\nu} v_s \delta \quad , \qquad \text{for } r_s \leq r \leq r_m \text{ , and} \tag{25}$$

where $\delta = \Delta a/a$. This expression, as shown earlier [11], is exact.

The second contribution stems from externally applied loads and loads generated by the gas pressure p inside the void and by the surface tension

Table 1. Parameters Used for the Void Capture Efficiency

Parameter	Symbol	Value
Shear Modulus	μ_m	10^5 MPa
Surface Stress	σ_s	0 or 1 J/m^2
Burgers Vector	b	2.5×10^{-10} m
Atomic Volume	Ω	b^3
Poisson's Ratio	ν	0.3
Relaxation Volume		
for interstitials	v_I	1.4 Ω
for vacancies	v_v	-0.2 Ω
Shear Polarizability		
for interstitials	α_I^G	-2.4×10^{-17} J
for vacancies	α_v^G	-2.4×10^{-18} J
Temperature	T	300, 450, 600°C

$2\sigma_s/r_s$, where σ_s is the surface stress. This contribution may be interpreted as being due to the stress-induced coherency strains. For the case wherethe external loads produce a purely hydrostatic stress σ_H, this contribution can be written as [11]

$$\Delta U^{\sigma} = v_m\sigma_H - v_s \frac{3\sigma_H(1-\nu)+(1-g)(1+\nu)(p-2\sigma_s/r_s)(r_s/r_m)^3}{3g(1-\nu)+(1-g)(1+\nu)(1-r_s^3/r_m^3)} \quad . \tag{26}$$

Further simplification of this expression is possible when $h<<r_s$ and $v_m = v_s = v$. Then

$$\Delta U^{\sigma} \cong (1-\frac{1}{g})v\{\sigma_H + \frac{1+\nu}{1-\nu}(\frac{2\sigma_s}{r_s} - p)\} \quad . \tag{27}$$

The total shell barrier is now given by

$$\Delta U^{*} = \Delta U^{o} + \Delta U^{c} + \Delta U^{\sigma} \quad , \tag{28}$$

and it constitutes a suitable approximation to the change of the total interaction energy of a point defect with a void as caused by the presence of a coating with different shear modulus.

Finally, there remains to be added to the long-range image interaction $U_o^I(r)$ a stress-induced interaction $U^{\sigma}(r)$. This long-range contribution was derived previously [14] for an arbitrary triaxial stress as generated by external loads. The general results obtained indicated, however, that the effect of the deviatoric stresses on the void capture efficiency is small in comparison with the effect of the hydrostatic stress. Hence, it suffices to use the expression derived for hydrostatic loading only, and it can be written as

$$U^{\sigma}(r) = \frac{3\alpha^{G}}{8\mu_m^2}\left(\frac{r_s}{r}\right)^6\left(\sigma_H + p + \mu_m\,\delta - \frac{2\sigma_s}{r_s}\right)^2 \tag{29}$$

where α^{G} is the shear polarizability of the point defect.

We summarize this section by stating that the total interaction energy of the point defect as it enters the drift term in Eq. (1) is given by

$$U^{S}(r) \cong \begin{cases} \Delta U^{*} + U_o^{I}(r) + U^{\sigma}(r) & \text{for } r_s \leq r \leq r_m \\ U_o^{I}(r) + U^{\sigma}(r) & \text{for } r \geq r_m \end{cases} . \tag{30}$$

This form of $U^{S}(r)$ is employed in the subsequent development of the void capture efficiency.

III. The Void Capture Efficiency

The void capture efficiency can be obtained by solving the steady-state diffusion equation $\underset{\sim}{\nabla} \cdot \underset{\sim}{j} = 0$. It was shown earlier [8] that for a spherically symmetric interaction $U^{S}(r)$, the capture efficiency (or bias factor) for a void is defined as

$$Z^{o} = \left\{\int_0^1 d(r_s/r)\, \exp[U^{S}(r)/kT]\right\}^{-1} . \tag{31}$$

The integration can be split into two parts, one over the region of the shell, and one over the matrix region. Accordingly, we write for the integral in Eq. (31)

$$\exp(\Delta U^{*}/kT) \int_{1/\eta}^{1} d(r_s/r)\, \exp[(U_o^{I} + U^{\sigma})/kT]$$

$$+ \int_0^{1/\eta} d(r_s/r)\, \exp[(U_o^{I} + U^{\sigma})/kT] \quad ,$$

where

$$1/\eta = 1/(1+h/r_s) \cong 1 - h/r_s \quad . \tag{32}$$

We may further write this as

$$\int_0^1 d(r_s/r)\, \exp[(U_o^I + U^\sigma)/kT]$$

$$+ [\exp(\Delta U^*/kT) - 1] \int_{1/\eta}^1 d(r_s/r)\, \exp[(U_o^I + U^\sigma)/kT] \quad .$$

The integrals contain only the long-range portions of the interaction. Therefore, the first integral is simply equal to $1/Z^b$, where Z^b is the capture efficiency or bias factor of a bare void without a shell. According to previous work [8,14], Z^b is given by

$$Z^b \cong 1 + (\frac{\Gamma_m}{kT})^{1/3} r_s^{-1} - \frac{3}{56} \frac{\alpha^G}{\mu_m^2 kT} (\sigma_H + p + \mu_m \delta - \frac{2\sigma_s}{r_s})^2 \quad . \tag{33}$$

The short-range or shell contribution to the bias is given by the second integral. It can be written as

$$\int_{1/\eta}^1 d(r_s/r)\, \exp[(U_o^I + U^\sigma)/kT] \cong \frac{h}{r_s} \exp[\bar{U}/kT] \quad , \tag{34}$$

where $\bar{U}$ is an appropriate average of $U_o^I + U^\sigma$ over the shell thickness. Since $(U_o^I + U^\sigma)$ is a monotonically decreasing function as the void surface is approached, its average $\bar{U}$ coincides with the exact value at a certain location with the shell. In the context of the above approximations, we may select for $\bar{U}$ the value of the interaction at $r = r_s + \rho$. Hence,

$$\bar{U} = U_o^I(r_s + \rho) + U^\sigma(r_s + \rho)$$

$$\cong -\frac{\Gamma_m}{\rho^3} + \frac{3\alpha^G}{8\mu_m^2}(\sigma_H + p + \mu_m\delta - \frac{2\sigma_s}{r_s})^2 \qquad (35)$$

where terms of order (ρ/r_s) in U^σ can be neglected because $h \ll r_s$.

We arrive then finally at a simple expression for the void capture efficiency:

$$\boxed{Z^o \cong \{\frac{1}{Z^b} + \frac{h}{r_s}\exp(\bar{U}/kT)[\exp(\Delta U^*/kT) - 1]\}^{-1}} \qquad (36)$$

Similar forms have been proposed earlier [8,10].

The equation (36) incorporates both cases for diffusion-limited as well as for surface-limited reaction rates. The former is obtained in the absence of a surface barrier, i.e., for $\Delta U^* = 0$. In this case, $Z^o = Z^b$. The surface-limited reaction rate is obtained when $(1/Z^b)$ is negligible compared to the second term in Eq. (36). In this case, Z^o becomes proportional to r_s, and since the defect current into the void is proportional to $Z^o 4\pi r_s$, the current is indeed dependent on $4\pi r_s^2$, the total surface area of the void.

IV. Results

For the numerical evaluation of Eq. (36), the parameters listed in Table 1 were used. They are considered to be applicable to nickel and to austenitic stainless steels. The chosen temperature range, from 300 to 600°C, covers the range where swelling occurs in a fast neutron flux.

In the following figures we show the ratio of the void capture efficiencies for interstitials and vacancies, i.e., Z_I^o/Z_v^o, as this is the

appropriate quantity for both void nucleation and void growth theories. This capture ratio depends on the void radius, r_s/b, the shell thickness, h/b, and the fractional difference in shear moduli, $1-g$.

For a shell which is two atomic layers thick, i.e., for $h = 2b$, Fig. 5 shows the void capture ratio as a function of the void radius and for different values of $(1-g)$. The band labelled with $1-g = 0$ represents this ratio for the bare void in the temperature range from 300° to 600°C. Furthermore, it was assumed that the surface stress σ_s, the gas pressure. p, the external hydrostatic stress σ_H, and the lattice mismatch δ are all zero. In this case $\overline{U}$ is independent of the void radius and relatively small. Therefore, when r_s/h is small, the surface barrier effect is dominant, and the void capture ratio is much smaller than one for $(1-g) \gtrsim 0.04$. However, as r_s increases the barrier effect diminishes, and the void capture ratio approaches unity. In general, we see from Fig. 5 that the effect of the barrier increases dramatically with only modest increases in the shear modulus of the shell. In fact, the increase in shear modulus relative to the matrix need be no more than a few percent.

The shell thickness (h/b) causes a similar reduction in the void bias ratio, as seen in Fig. 6. Here, as in the example of Fig. 5, the parameters σ_s, p, σ_H, and δ are all zero, and $1-g = 0.01$.

If we now assume that a surface stress exists of value $\sigma_s = 1 J/m^2$, the stress-induced interaction counteracts the surface barrier when the voids are small. This is shown in both Fig. 7 and Fig. 8. In the case of Fig. 7, $h = 2b$, and $(1-g)$ is varied, whereas for the case of Fig. 8, $(1-g) = 0.01$ and h/b is changed. In contrast to the corresponding results of Figs. 5 and 6, we see that for very small vacancy

clusters the long-range stress-induced interaction dominates the void capture ratio. The reason for this can be found in the energy $\overline{U}$. According to Eq. (34), $\overline{U}$ becomes increasingly negative with decreasing r_s when $\sigma_s \neq 0$ because α_I^G is negative. As a result, the second term in the bracket of Eq. (36) becomes small, and the void capture efficiency approaches the expression Z^b for a bare void.

Since impurity segregation to surfaces and to sinks is the likely cause for the formation of a void shell it is reasonable to assume that during nucleation the void shell increases its thickness in proportion to the void radius r_s. In order to model this, we assume that

$$h = b + f\, r_s \tag{37}$$

where f is a fractional number smaller than one. For f = 0, or h = b, one obtains essentially the same capture efficiency as for the bare void. The first term in Eq. (37) was only added to avoid numerical difficulties when f approaches zero.

For a void shell with a thickness increasing with the void radius, the void capture ratio is shown in Fig. 9 for the case of T = 450°C and (1-g) = 0.05. Initially, this ratio follows the one for the bare voids when the void radius or the shell thickness is small. However, when the shell thickness has grown to two atomic layers the void capture ratio decreases rapidly with increasing radius. This transition from diffusion to surface-reaction controlled growth is shifted somewhat when (1-g) is varied, as shown in Fig. 9. Here, the fraction f was assumed to be 0.1 (and T = 450°C).

V. Discussion

Segregation of impurities or alloying elements to a vacancy cluster or embryonic void has been shown to have a profound effect on the capture efficiencies for interstitials and vacancies. When the segregation leads to a shell with a shear modulus only slightly higher than in the surrounding matrix, the void becomes a highly preferential sink for vacancies. It not only loses its preferential capture efficiency for interstitials, but it becomes biased against interstitials.

This reversal of the "void bias" has important implications for void nucleation as mentioned previously [9,10,15]. In the absence of a void shell, the image interaction U_o^I causes the void to preferentially capture interstitials. Void nucleation without the assistance of insoluble gases is suppressed. Nevertheless, there exists a subcritical population of void embryos during irradiation. Only those embryos which acquire a shell will grow to supercritical size. Therefore, void nucleation is determined by the rate of segregation to the subcritical void embryos. Of course, the segregation must produce a shell with slightly higher shear modulus. If the shell had a lower shear modulus, the void embryo would eventually disappear again as a result of the preferential interstitial capture.

One of the important conclusions which transcends the particular theme of this paper is that one must add the relaxation energy U^R of the crystal defect to its mechanical interaction energy in order to obtain the total mechanical energy. In a stress free crystal, this energy can be written as the sum of two parts, $U^R + U^I$. The image interaction U^I is in effect nothing else but the change in the relaxation energy

when the defect is located close to a free surface or an interface, so that $(U^R + U^I)$ is the local relaxation energy. The recognition of this fact has three important implications which we believe are also valid for other crystal defects, e.g., dislocations.

First, the total energy changes continuously and monotonically when the defect traverses a coherent interface between two media with different elastic properties. No discontinuity or oscillatory variation occurs at the interface.

The second implication is that the singularity in U^I at the interface, being a mathematical artifact, can be removed by introducing a cut-off distance measured from the interface or the free surface, beyond which the image interaction U^I is valid. By virtue of the requirement for monotonic change of $(U^R + U^I)$, this cut-off distance can be uniquely defined.

The third implication pertains to the question of how distinct a coherent interface must be in order to give rise to an image interaction U^I. As we have shown, the image interaction simply creates a gradual transition of the total relaxation energy $(U^R + U^I)$ for a sharp interface. On the other hand, if interdiffusion produces a gradual transition from one medium to the other, the relaxation energy U^R would by itself change gradually. Hence, we can conclude that regardless of the sharpness of the interface, the total relaxation energy $(U^R + U^I)$ always changes gradually, either because of U^I or because of a continuous change in alloy composition. As a consequence, the derived results for the capture efficiencies of coated voids remain essentially valid even if the void shell region does not clearly distinguish itself from the matrix material by a sharp interface but rather by a gradual concentration gradient of segregated impurities.

We have mentioned in Section II that the activation energy for defect migration, U^M, may also be a function of position. In fact, we have included this effect in our analysis through Eq. (2), but only derived changes in U^M of mechanical origin. There may be other factors which contribute to a change in U^M. For example, there may exist a binding energy between vacancies and impurity atoms segregated to the voids, and U^M may be enhanced by ΔU^M within the void shell region. By virtue of Eq. (3), we may include this effect by enhancing U^S and thereby increase ΔU^* by ΔU^M. Therefore, our Eq. (36) also encompasses the alteration of the diffusion coefficients near the void.

Segregation of impurities is not only restricted to voids, but takes place at all sinks. The dramatic effect this segregation has on the void capture efficiency leads us to suspect a similar effect on the dislocations and dislocation loops. The present analysis should be helpful in guiding future attempts to solve the more difficult problem of the capture efficiency of dislocations decorated by impurity clouds or precipitates.

Acknowledgement

Partial support for this work was provided by the Division of Basic Energy Sciences, U.S. Department of Energy, under contract ER-78-S-02-4861 with the University of Wisconsin.

References

[1] E. E. Bloom, J. O. Stiegler, A. F. Rowcliffe, and J. M. Leitnaker, Scripta Met. 10, 303 (1976).

[2] W. G. Johnston, T. Lauritzen, H. H. Rosolowski, and A. M. Turkalo, in Radiation Damage in Metals, eds., N.L. Peterson and S.D. Harkness, Amer. Soc. for Metals, Metals Park OH, 227 (1975).

[3] L. K. Mansur, in Proceedings of the Workshop on Correlation of Neutron and Charged Particle Damage, held June 8, 9, 1976, at Oak Ridge National Laboratory, CONF-760673.

[4] J. O. Stiegler, ed.; Proc. Workshop on Solute Segregation and Phase Stability during Irradiation, J. Nucl. Mater. 83, No. 1 (1979).

[5] P. R. Okamoto and H. Wiedersich, J. Nucl. Mater. 53, 336 (1974).

[6] K. Farrell, D. N. Braski, and J. Bently, submitted to Scripta Metallurgica.

[7] A. D. Brailsford, J. Nucl. Mater. 56, 7 (1975).

[8] W. G. Wolfer, in "Fund. Aspects of Radiation Damage in Metals," Proc. of an Internat. Conf., Gatlinburg, Oct. 1975, CONF-751006-P2, p. 812.

[9] L. K. Mansur and W. G. Wolfer, J. Nucl. Mater. 69/70, 825 (1978).

[10] L. K. Mansur and W. G. Wolfer, Oak Ridge National Laboratory Report, ORNL/TM-5670, Sept. 1977.

[11] W. G. Wolfer and L. K. Mansur, Phys. Stat. Sol. (A), 37, 211 (1976).

[12] J. D. Eshelby, Solid State Phys. 3, 79 (1956)

[13] B. Michel, Phys. Stat. Sol. (B) 81, K87 (1977).

[14] W. G. Wolfer and M. Ashkin, J. App. Phys. 46, 547 (1975).

[15] W. G. Wolfer, L. K. Mansur, and J. A. Sprague, in "Rad. Effects in Breeder Reactor Structural Materials", M. L. Bleiberg and J. W. Bennett (eds.), The Metallurgical Soc. of AIME, 1977, p. 479.

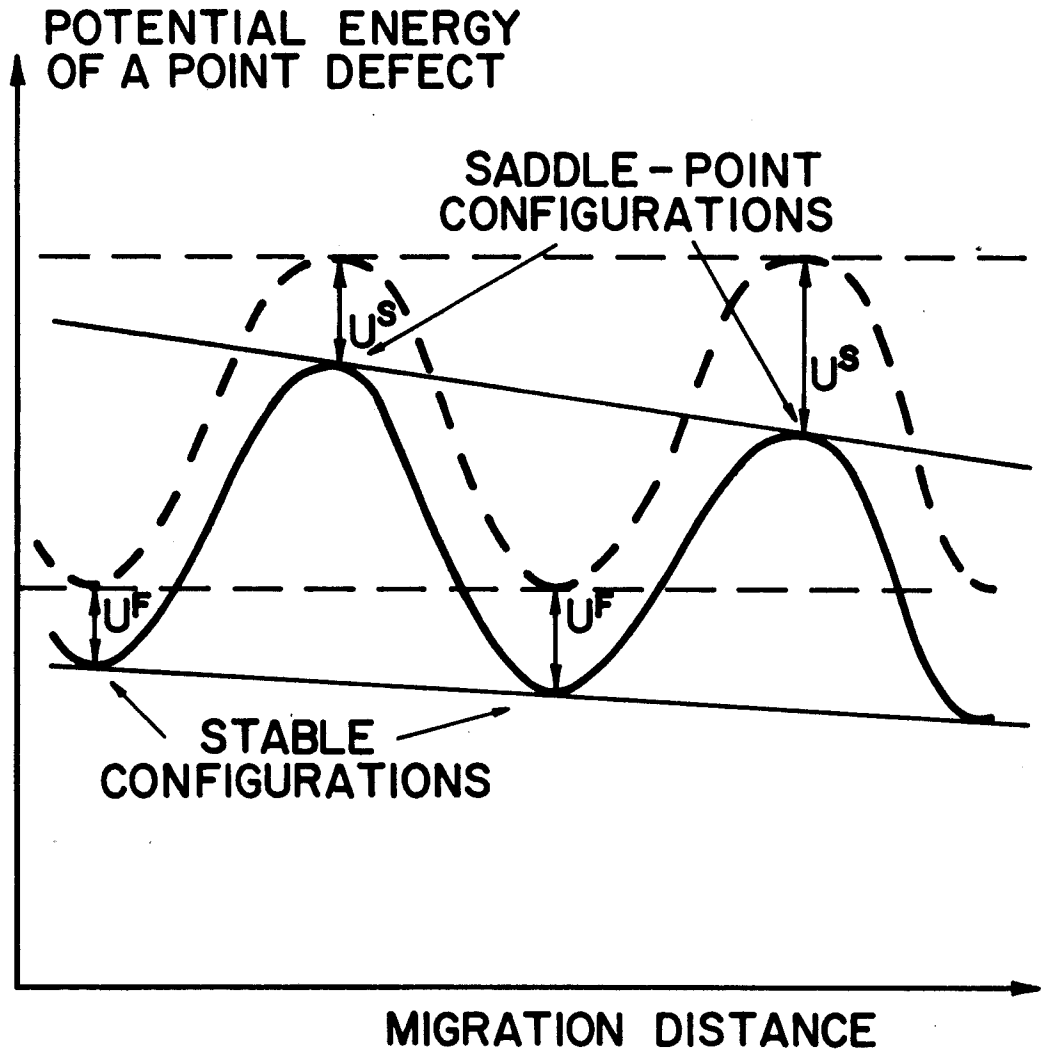

Fig. 1. Potential energy variation of a migrating point defect in an ideal (dashed curve) and an elastically deformed (solid line) lattice.

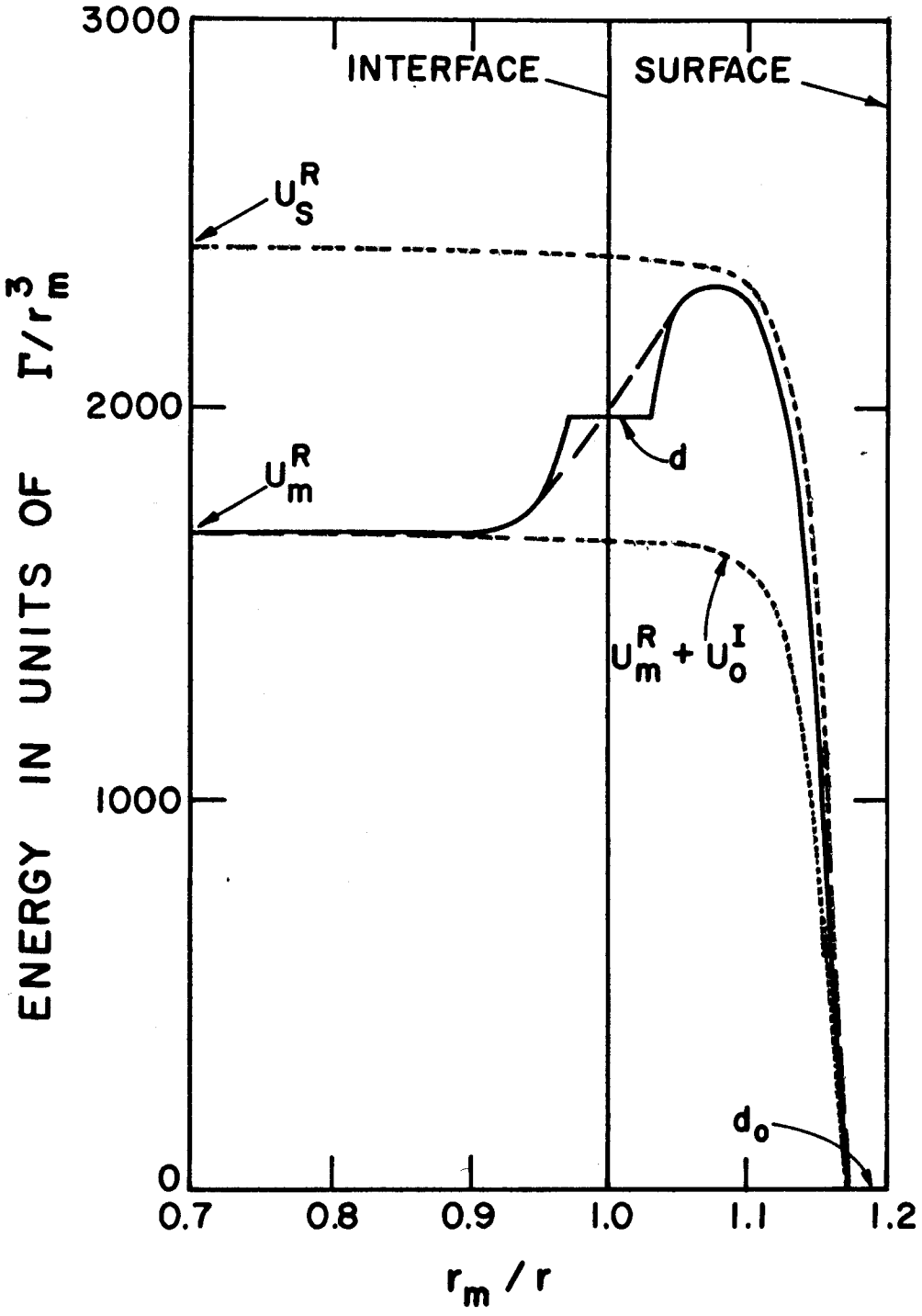

Fig. 2. The total strain energy ($U^R + U^I$) of a point defect in the vicinity of a coated void.

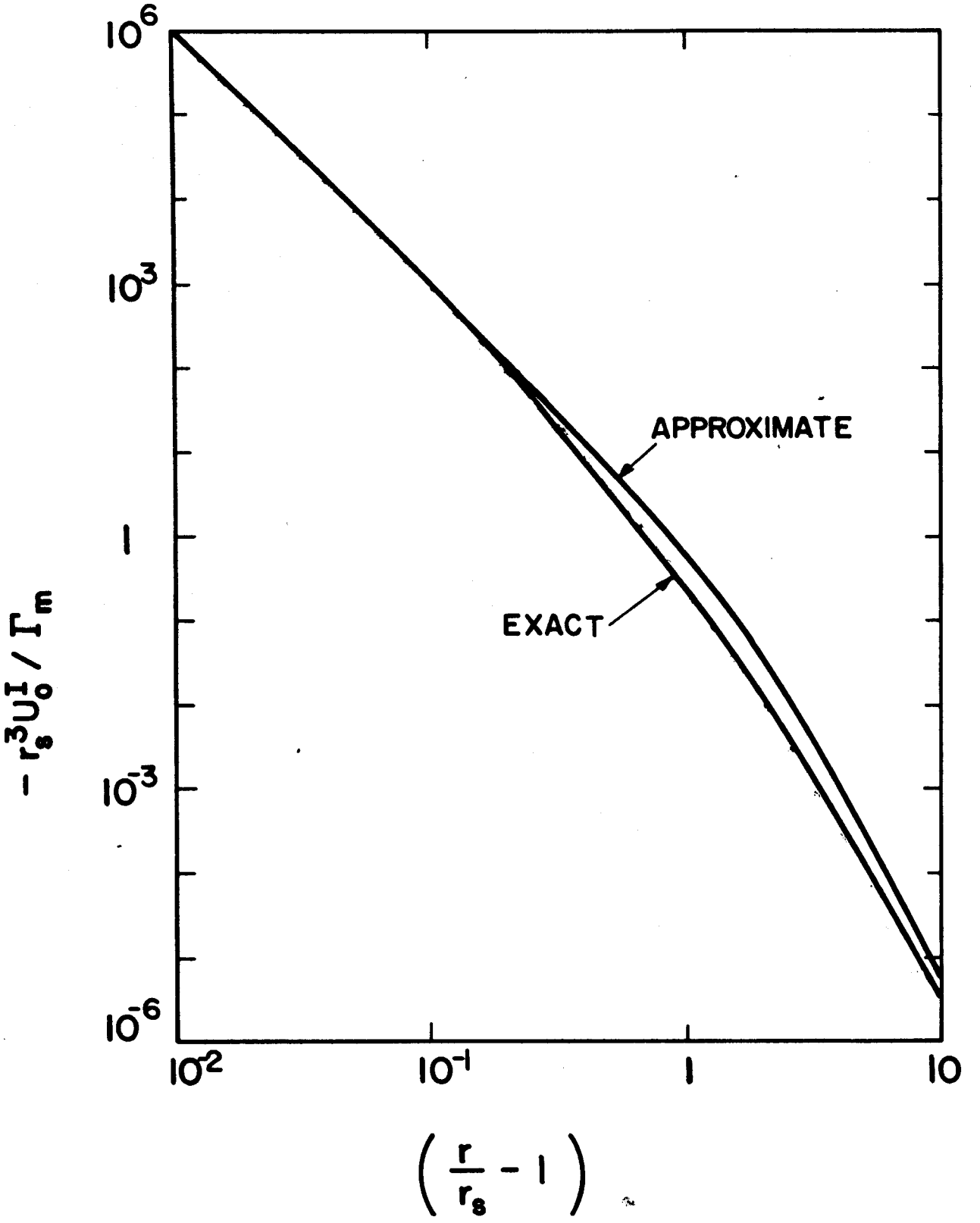

Fig. 3. Image interaction of a point defect with a bare void.

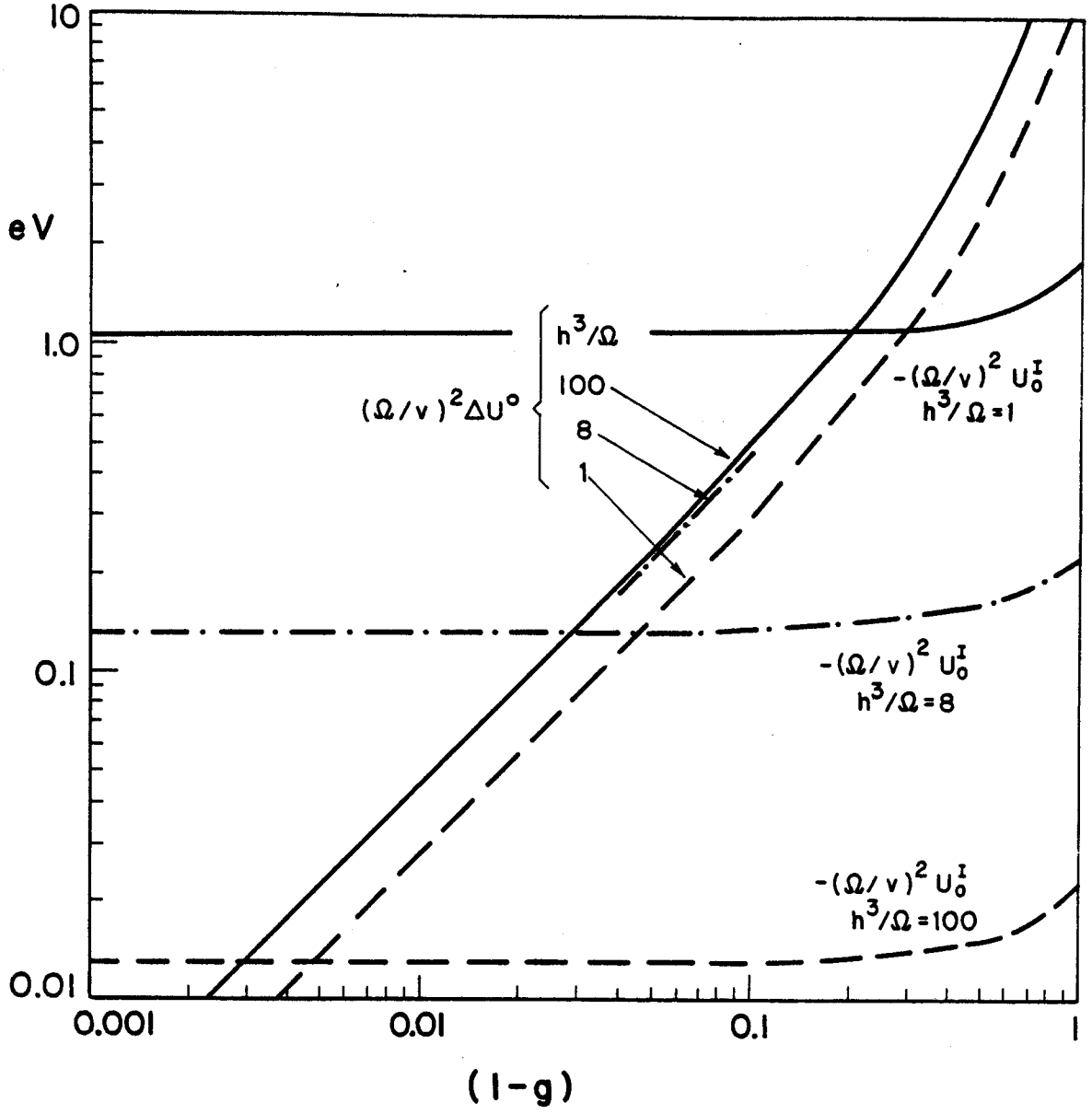

Fig. 4. Shell barrier energy, ΔU^{o}, and image interaction U_{o}^{I} within the shell.

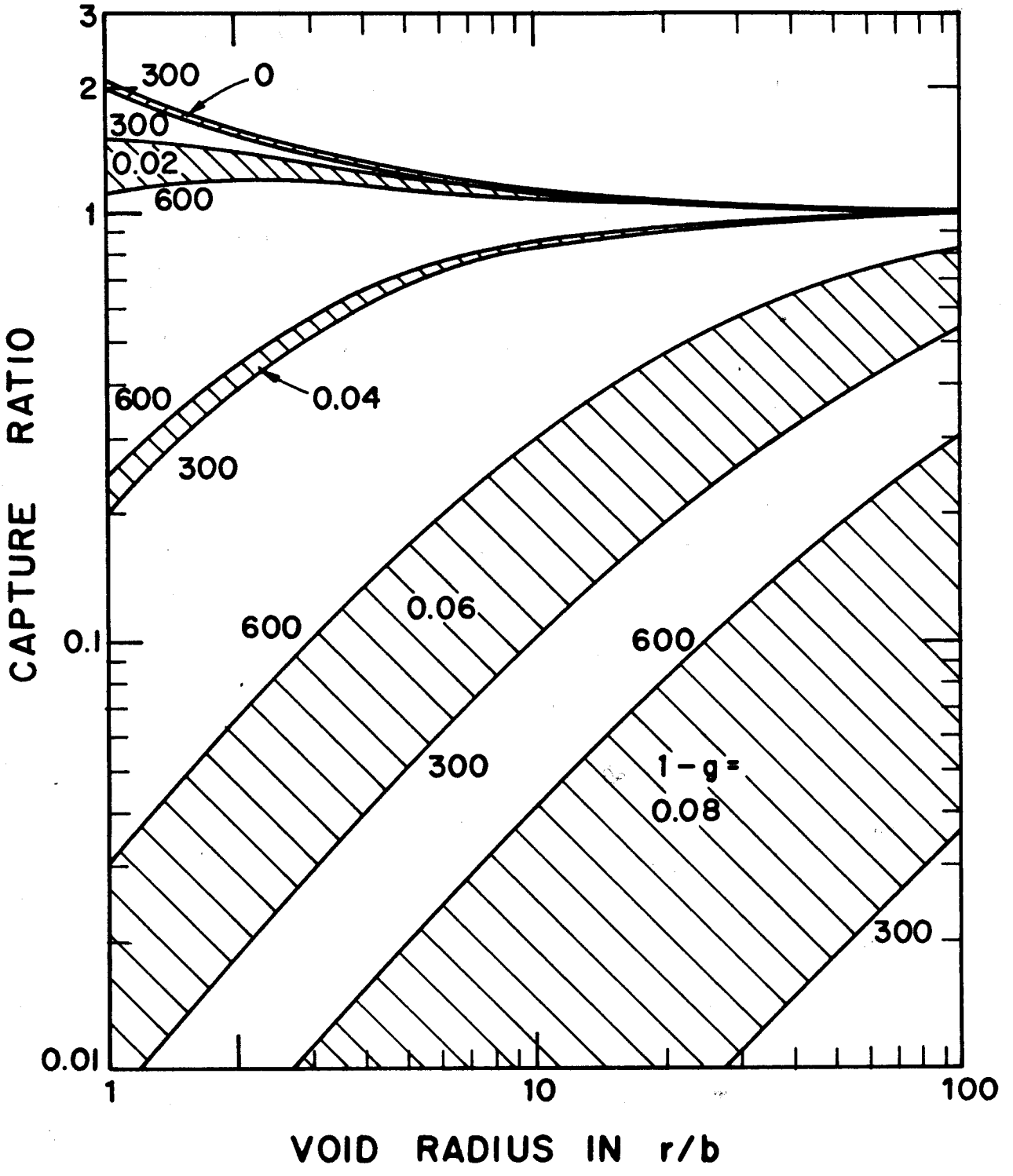

Fig. 5. Capture ratio Z_I^o/Z_V^o for coated voids with a shell thickness of h = 2b and zero surface stress.

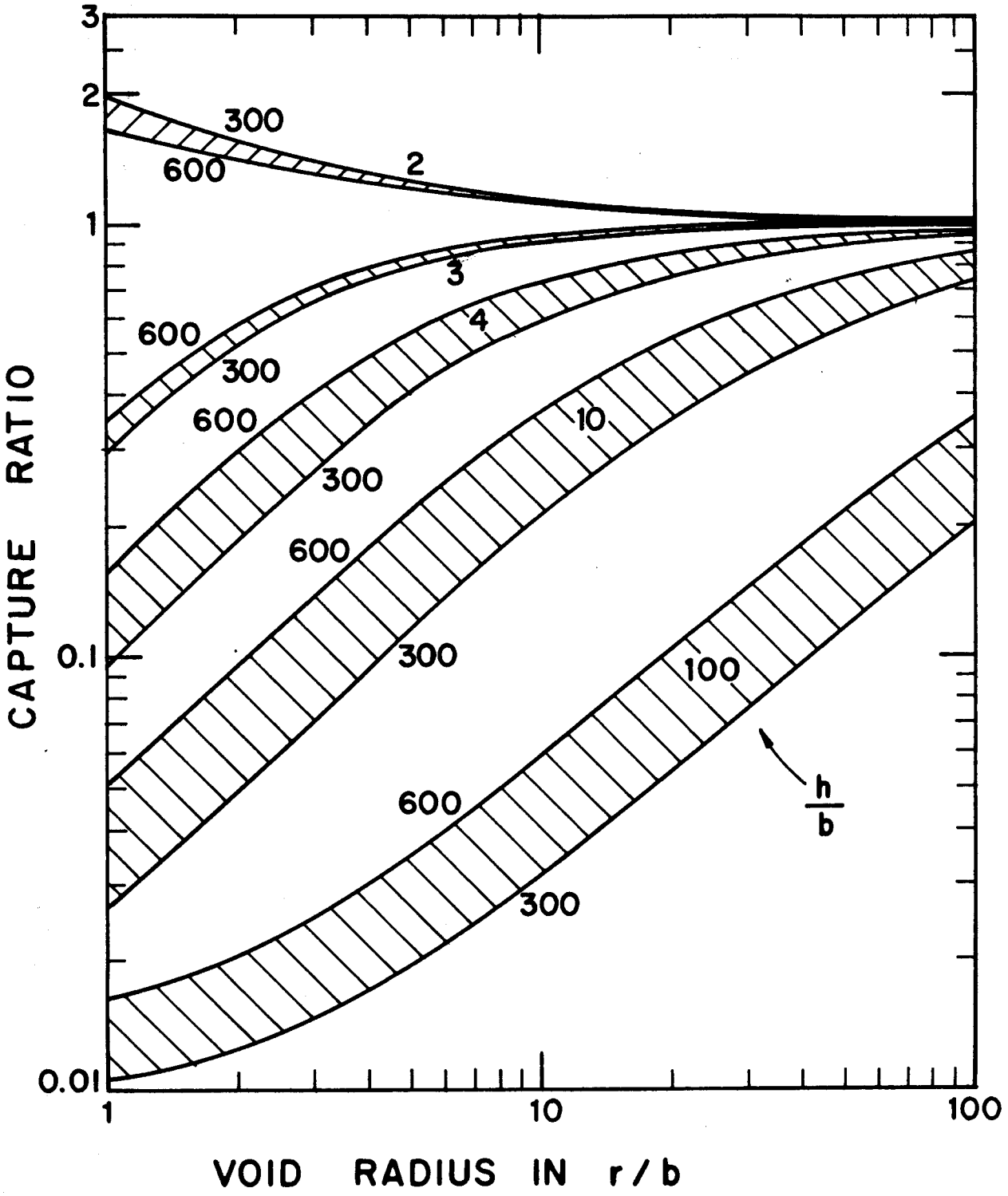

Fig. 6. Capture ratio Z_I^o/Z_V^o for coated voids of varying thickness; (1-g) = 0.01 and σ_s = 0.

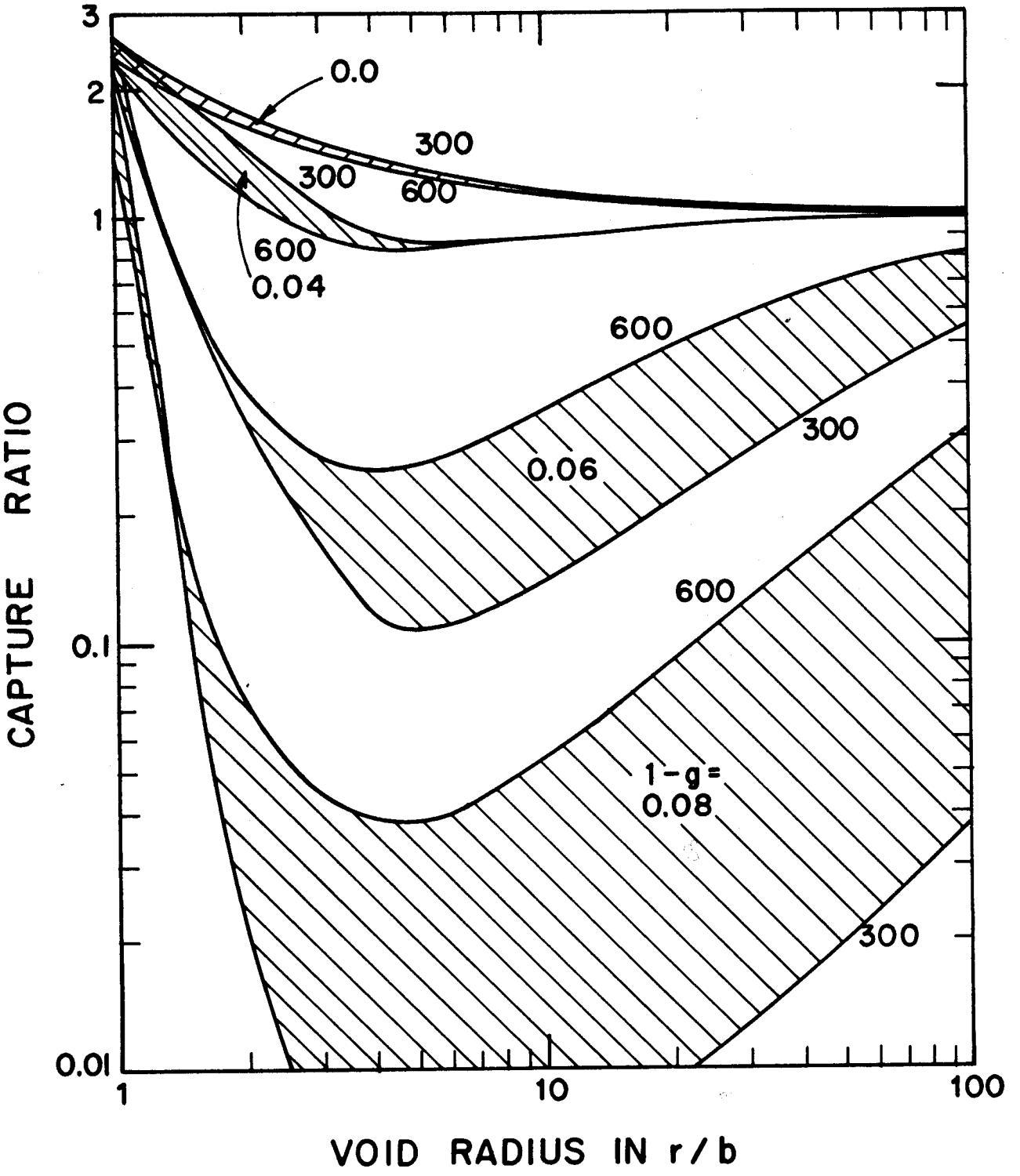

Fig. 7. Capture ratio Z_I^o/Z_V^o for coated voids with a shell thickness of $h = 2b$ and with a surface stress of $\sigma_s = 1 J/m^2$.

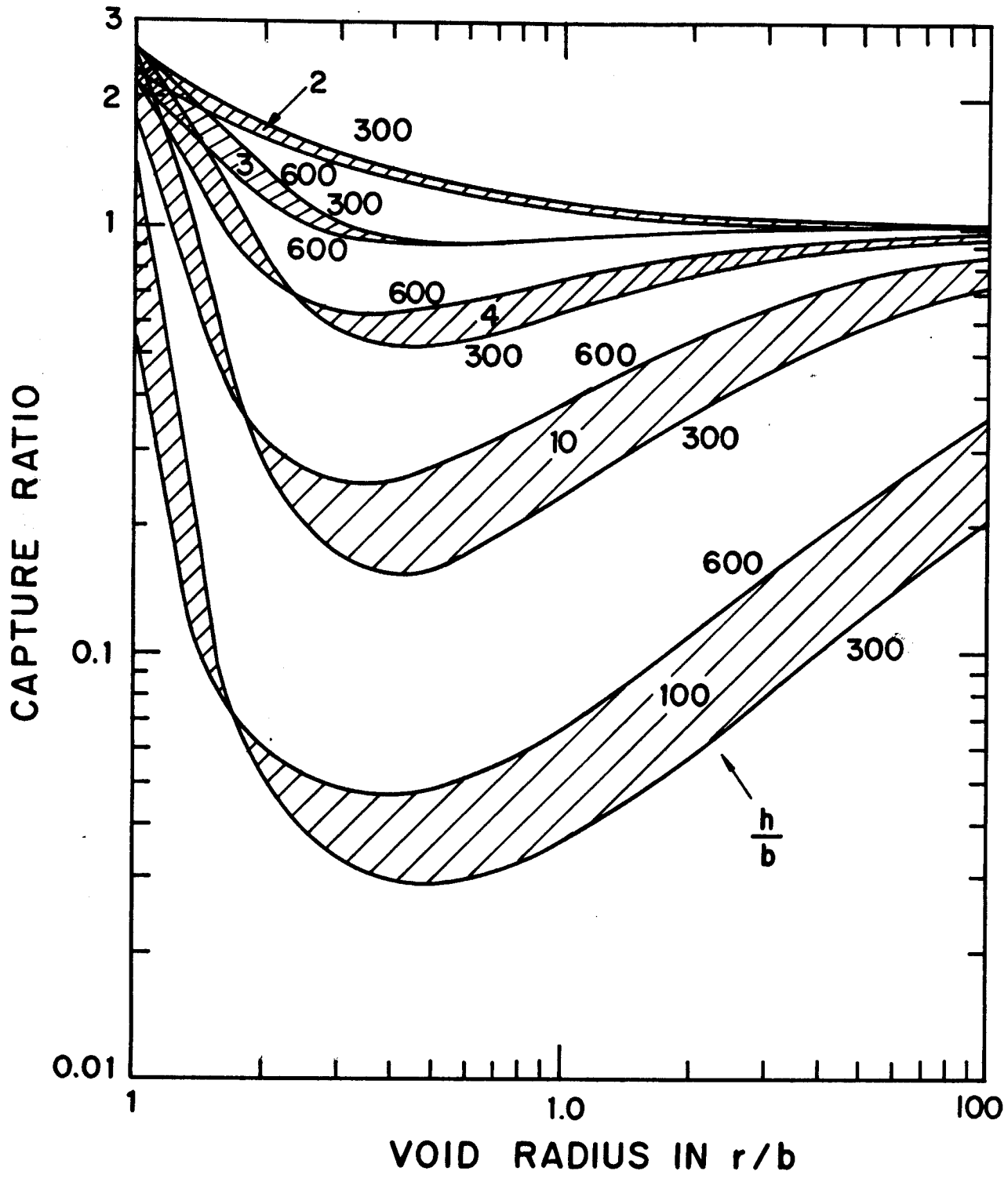

Fig. 8. Capture ratio Z_I^o/Z_V^o for coated voids of varying thickness; (1-g) = 0.01 and σ_s = 1J/m^2.

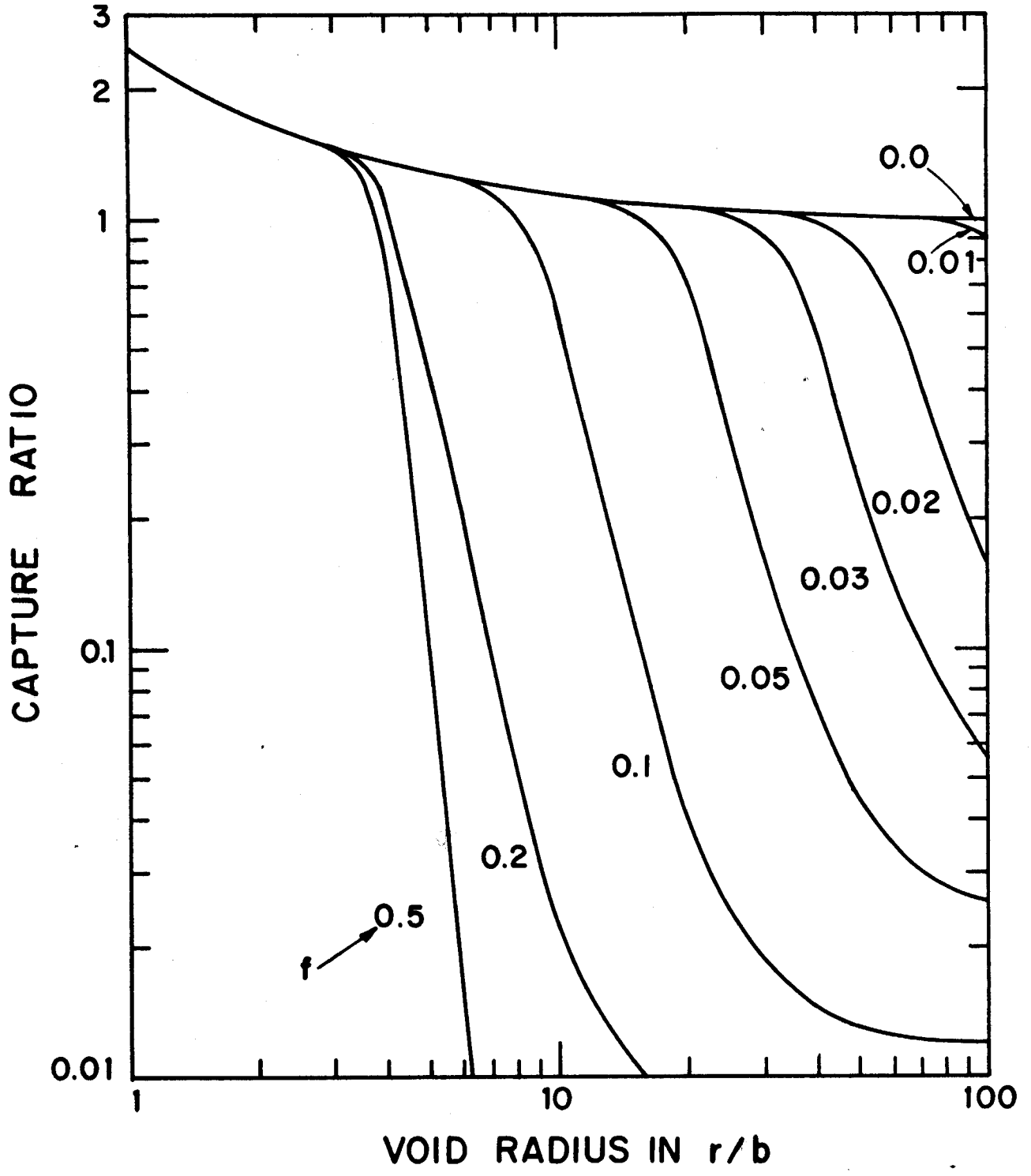

Fig. 9. Capture ratio Z_I^o/Z_V^o for voids with shell thickness increasing with the void radius; (1-g) = 0.05, T = 450°C, σ_s = 1J/m^2.

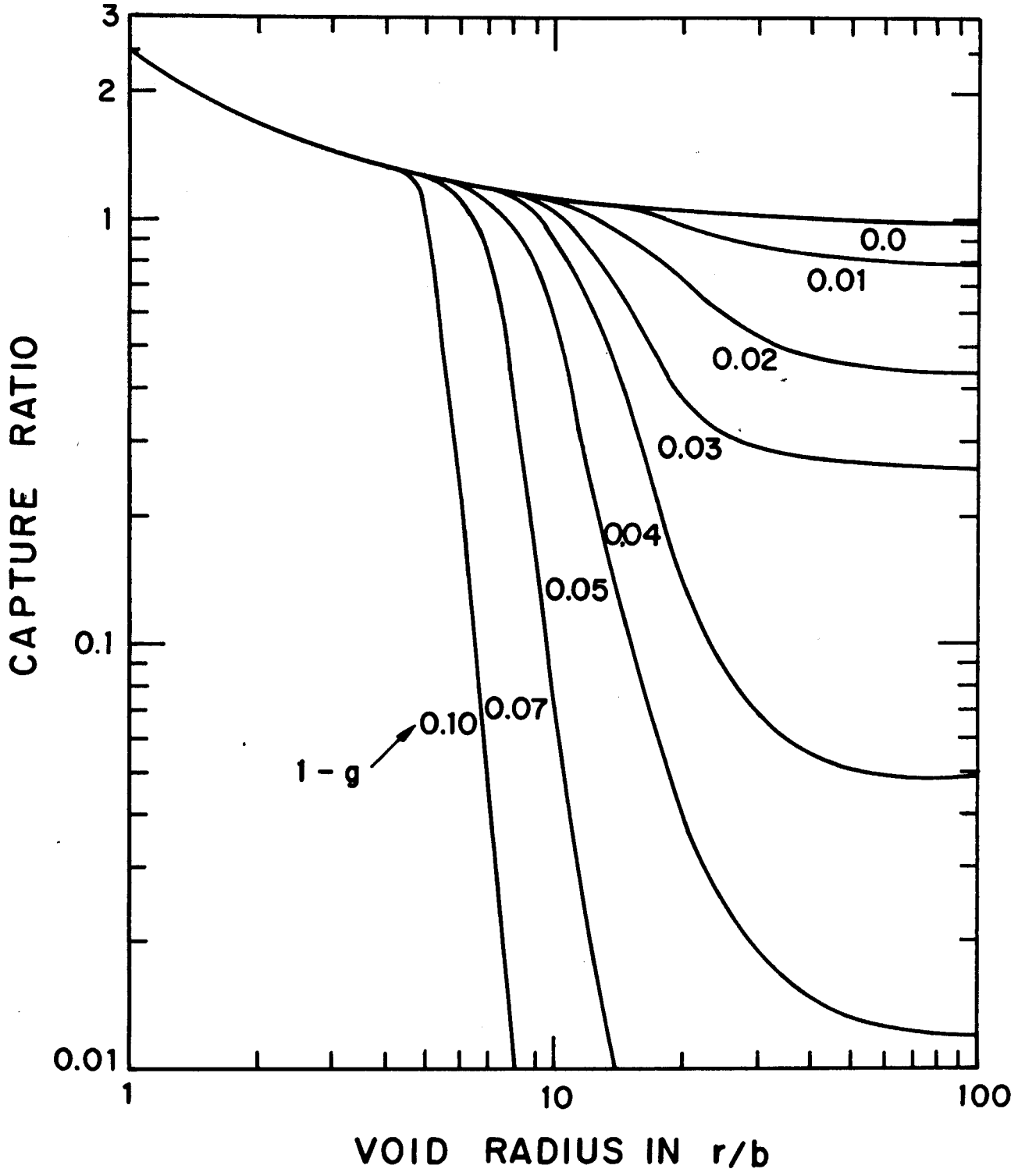

Fig. 10. Capture ratio Z_I^o/Z_V^o for voids with a shell thickness equal to 10% of the void radius, T = 450°C, σ_s = 1J/m^2.